

Ising anyonic topological phase of interacting Fermions in one dimension

K. Guther,* N. Lang, and H. P. Büchler

*Institute for Theoretical Physics III and Center for Integrated Quantum Science and Technology,
University of Stuttgart, Pfaffenwaldring 57, 70550 Stuttgart, Germany*

(Dated: March 7, 2024)

We study a microscopic model of interacting fermions in a ladder setup, where the total number of particles is conserved. At a special point, the ground state is known and gives rise to a topological state of matter with edge modes obeying the statistics of Ising anyons. Using a combination of bosonization as well as full scale numerical density-matrix renormalization group analysis, we map out the full phase diagram. We find that the topological phase survives in an extended parameter regime. Remarkably, an additional symmetry is required to protect the topological phase.

PACS numbers: 42.50.Nn, 32.80.Ee, 34.20.Cf, 42.50.Gy

The potential of low-dimensional quantum systems to exhibit topological order and host quasiparticles with anyonic statistics marks one of the most fascinating phenomena in condensed matter physics. The theoretical description of such systems [1, 2] and their potential applications to fault-tolerant quantum computation [3, 4] sparked the search for their realization in condensed matter setups and cold atomic gases. Prominent examples featuring non-abelian anyons are topological p -wave superconductors within their mean-field description [5–7], for which the existence of Majorana bound states in one [6] and two dimensions [8, 9] has been shown. Notably, recent experiments revealed signatures consistent with Majorana zero-energy edge-modes in nanowires [10–15]. However, a complete picture of Majorana modes in a particle conserving setup (i.e., beyond mean-field), and its competition with the gapless Goldstone mode in one-dimension, remains an open challenge. Especially for cold atomic gases, the need for a microscopic, number-conserving theory is expected to be of paramount importance.

Several theoretical studies have focused on the understanding of Majorana-like edge modes in one-dimensional systems beyond mean field theory. A prominent approach is based on effective low-energy theories employing bosonization [16–20], while the first exact solution has been restricted to models requiring unphysical long-range interactions [21]. Alternatively, one-dimensional double wire setups of spinless fermions with pair-correlated hopping have emerged as promising candidates: First, numerical studies have demonstrated the appearance of edge states in such a model [22]; later, exactly solvable extensions have been found [23, 24] and the Ising anyonic statistics of the edge states was demonstrated microscopically [23]. At this exactly solvable point, the topological properties are protected in generic wire networks by particle number conservation alone. However, it is not yet established whether this topological state extends over a finite parameter regime, and whether particle conservation is enough to protect the topological phase in general; the latter is of special interest as previous approaches by

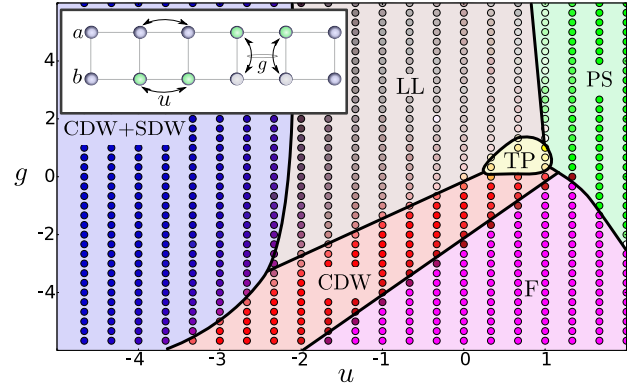


FIG. 1. *Phase diagram.* Numerical results for the phase diagram at half filling with system length $L = 50$ and $w = 1$. The dots represent pairs (u, g) for which the ground state was computed. The color encodes the respective phase: (PS) Intra-chain phase separation, (F) Inter-chain phase separation, (LL) Gapless Luttinger liquid with algebraic correlations, (TP) Topological phase with p -wave pairing, (CDW) Charge density wave due to a gap in the symmetric sector, (CDW+SDW) Charge- and spin density waves due to gaps in both sectors. The inset illustrates the double wire setup, highlighting the intra- and inter-chain density-density interactions. The dotted line indicates the extent of the topological phase at filling $\rho = 0.35$. Then it includes the point $g = u = 0$ studied in Ref. [22]. For a quantitative description of the color code, see the appendix.

bosonization revealed an algebraic splitting [17, 19] in absence of a local symmetry.

In this work, we derive the full ground state phase diagram of a microscopic model with spinless fermions on a double wire setup which contains both the analytically solvable Hamiltonian from [23] and the Hamiltonian employed in [22] as special cases. Using the combination of bosonization for a qualitative description of the phase diagram as well as a full scale numerical density-matrix renormalization group (DMRG) analysis, we bridge the gap between the previous approaches, present the full phase diagram and demonstrate the stability of the topological phase. In particular, we find that the previ-

ously studied models belong to the same phase and are smoothly connected to each other. We investigate the stability of the topological phase under perturbations. Especially, we find that perturbations violating the subchain parity and time-reversal symmetry lead to an algebraic splitting of the edge modes. This implies that even in a particle conserving setting the topological phase still belongs to the class which can be protected by either subchain parity or time-reversal symmetry.

Model: We start with the microscopic Hamiltonian describing spinless fermions on a one-dimensional double chain. The chain consist of L lattice sites, and a_i^\dagger (b_i^\dagger) denotes the fermionic creation operators on the upper (lower) chain at lattice site i . The Hamiltonian involves nearest-neighbor hopping, interactions within each chain and interactions between the chains. It is conveniently written as

$$H = \sum_i \sum_{\sigma \in \{a,b\}} \left[-A_i^\sigma + u (A_i^\sigma)^2 \right] + \left[wB_i + gB_i^2 \right] \quad (1)$$

with the single-particle hopping within each chain

$$A^a = a_i^\dagger a_{i+1} + a_{i+1}^\dagger a_i \quad \text{and} \quad A^b = b_i^\dagger b_{i+1} + b_{i+1}^\dagger b_i. \quad (2)$$

The second term describes a nearest-neighbor attraction within each chain as well as a shift in chemical potential, i.e.,

$$(A_i^\sigma)^2 = n_i^\sigma + n_{i+1}^\sigma - 2n_i^\sigma n_{i+1}^\sigma,$$

with $\sigma \in \{a,b\}$. Here, n_i^σ is the number of fermions on site i of chain σ . Furthermore, the interaction *between* the chains is given by the pair-correlated hopping

$$B_i = a_i^\dagger a_{i+1}^\dagger b_i b_{i+1} + b_i^\dagger b_{i+1}^\dagger a_i a_{i+1}. \quad (3)$$

Note that the sign of w can be changed by the gauge transformation $a_j \mapsto ia_j$. In the following, we hence restrict the analysis to $w > 0$. The last term in (1) describes an inter-chain interaction and involves up to four-body interactions between the fermions

$$B_i^2 = n_i^a n_{i+1}^a (1 - n_i^b)(1 - n_{i+1}^b) + [a \leftrightarrow b]$$

For simplicity, we fixed the particle tunneling within the chains to unity and express all energies in terms of this tunneling energy. In addition to the conservation of the total particle number N , this Hamiltonian exhibits time-reversal symmetry (represented by complex conjugation) and conserves the fermionic subchain parity; the latter is denoted as $\alpha = \pm 1$ for an even (odd) number of fermions on the upper chain. The Hamiltonian allows for an exact derivation of the ground states if $u = 1$ and $w = g \geq 0$, where the appearance of a robust ground state degeneracy characterized by the subchain parity α as well as topological edge modes with Ising anyonic braiding statistics has been demonstrated [23]. Notably,

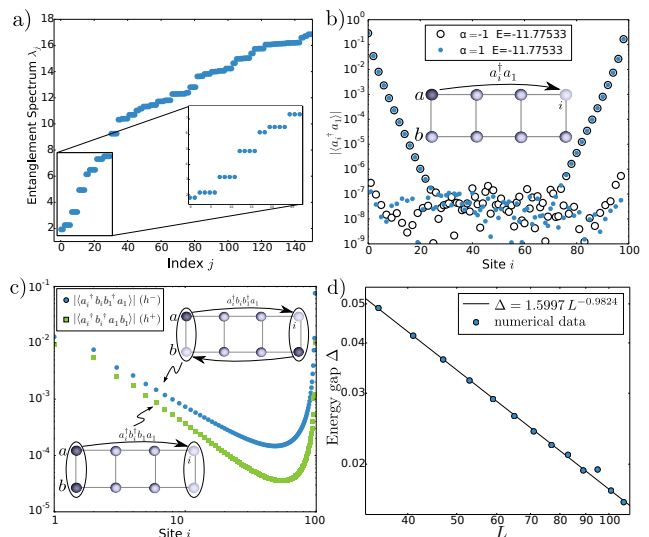


FIG. 2. *Topological phase.* (a) Entanglement spectrum for a ladder of length $L = 100$ with open boundaries and parameters $u = g = 0.9$ and $w = 1$ at half filling with $\alpha = 1$ for a bipartition at site 40. The energy accuracy for the numerically determined approximate ground state is $\frac{\Delta E}{|E|} = 2.6 \cdot 10^{-4}$. The twofold degeneracy is an indication of topological order. (b) On-chain Green's function of this system featuring exponential decay and a revival at the other end of the chain, indicating the existence of a localized edge state. For $\alpha = -1$, it is $\frac{\Delta E}{|E|} = 3.1 \cdot 10^{-4}$. Note that the agreement in the ground state energy goes beyond accuracy because the energy error is expected to be the same for both states. (c) Inter-chain two-point correlation functions of the same state exhibiting algebraic behaviour and also a revival at the other end of the chain. (d) Scaling of the energy gap Δ in the topological phase for $u = g = 0.9$ and $w = 1$ in the $\alpha = -1$ sector at half filling for open boundaries.

the ground state is the equal-weight superposition of all states with fixed total particle number N and fermionic subchain parity α . The intuitive interpretation is the following: The combination of intra-chain attraction with pair-hopping gives rise to p -wave pairing. Then, naively, each wire acts as a mean-field superconductor for the other one and allows for its description as Majorana chain [6]. Remarkably, this picture remains valid despite the quasi long-range order in one-dimension.

At $u = 0 = g$, the model has previously been studied numerically with DMRG [22] where the appearance of edge modes has been observed away from half filling $\rho = N/2L \neq 1/2$. Therefore, Hamiltonian (1) can interpolate between the exactly solvable point of [23] and the Hamiltonian describing a possible realization of a topological superconductor in cold atomic gases in [22].

Methods: We analyze the ground state phase diagram with two different methods: In order to obtain a qualitative understanding of potentially competing phases, we apply the conventional bosonization methods [25, 26] to obtain an effective low-energy field theory for the contin-

uum limit of the model. On the other hand, we pin down the precise values for the phase transitions by performing a full scan of the phase diagram using DMRG.

We start with the description of the bosonization procedure as reviewed in [27]: The fermionic field operators ψ_σ of chain $\sigma \in \{a, b\}$ in the continuum are decomposed into left- and right-moving modes $\psi_{\sigma R/L}$ as

$$\psi_\sigma(x) = \psi_{\sigma R}(x) e^{ik_F x} + \psi_{\sigma L}(x) e^{-ik_F x}. \quad (4)$$

Here, $k_F = \pi\rho$ is the Fermi-wavenumber defining the filling fraction ρ . The gist of bosonization is the expression of $\psi_{\sigma R/L}$ in terms of the bosonic density field ϕ_σ and the phase field θ_σ via

$$\psi_{\sigma R/L} = \frac{\eta_{\sigma R/L}}{\sqrt{2\pi}} : e^{-i\sqrt{\pi}(\theta_\sigma \pm \phi_\sigma)} :. \quad (5)$$

Here, $\eta_{\sigma R/L}$ are Klein factors ensuring the anticommutation of different fermion operators, and $: \bullet :.$ denotes normal ordering. It is convenient to introduce bosonic fields which are symmetric and antisymmetric with respect to chain exchange $a \leftrightarrow b$ [16],

$$\phi_\pm = \frac{1}{\sqrt{2}} (\phi_a \pm \phi_b), \quad \theta_\pm = \frac{1}{\sqrt{2}} (\theta_a \pm \theta_b). \quad (6)$$

The term of the Hamiltonian responsible for the topological phase separates with respect to these sectors. We then expand the full theory (1) around the non-interacting point $u = g = w = 0$ which is described by two decoupled Luttinger liquids. The qualitative picture of the phase diagram follows from renormalization group arguments: Including interactions leads to renormalized Luttinger parameters K_\pm and, more importantly, provides potentially relevant terms which characterize transitions into new phases; they will be discussed below.

For the quantitative mapping of the phase diagram, we study the model numerically using the well-established DMRG algorithm [28, 29] in its formulation as a variational matrix product state ansatz [30]. Our implementation is tailored to Hamiltonian (1) and allows for the efficient computation of ground- and low lying excited states, exploiting the $U(1)$ symmetry (particle conservation) and the \mathbb{Z}_2 symmetry (subchain parity). To avoid local minima and enhance convergence, we employ subspace expansion [31]; see the appendix for the utilized libraries.

Phase diagram: We start analyzing the phase diagram at half filling, $N = L$, in the vicinity of the exactly solvable point $u = g = w = 1$. The **topological phase** (TP) is identified by three characteristic properties: (i) a robust ground state degeneracy with respect to the subchain parity α , (ii) the existence of exponentially localized edge states manifest in a revival of the otherwise exponentially decaying on-chain Green's function $\langle a_i^\dagger a_1 \rangle$ at the end of the chain, and (iii) a double degeneracy of the entanglement spectrum. In Fig. 2 (a-b), we show

DMRG results for these properties at a generic point inside the topological phase.

These observations are in agreement with the qualitative results for the bosonized theory: Inter-chain pair hopping gives rise to the operator

$$\psi_{Ra}^\dagger \psi_{La}^\dagger \psi_{Lb} \psi_{Rb} + \text{h.c.} \propto \cos\left(\sqrt{8\pi/K_-} \theta_-\right), \quad (7)$$

which becomes relevant for $K_- > 1$. Then it is responsible for opening an energy gap in the asymmetric sector by pinning the relative phase θ_- to the values $\pm\sqrt{K_-}\pi/8$. As shown in Ref. [16], the resulting effective theory describes a topological phase and can be refermionized to the continuum version of the Majorana chain [6] at the Luther-Emery point $K_- = 2$. Note that an alternative approach for a topological phase has been studied in Ref. [20], where the relevant term involves the density field ϕ_- which corresponds to an interaction conserving the number of particles on each wire. The topological phase in the present manuscript directly connects to the exactly solvable, critical point for which the edge states have Ising anyonic braiding statistics [23]. This interpretation is confirmed by the numerical evaluation of the pair-correlation functions $h^-(x) = \langle \psi_a^\dagger(x) \psi_b(x) \psi_b^\dagger(0) \psi_a(0) \rangle$ and $h^+(x) = \langle \psi_a^\dagger(x) \psi_b^\dagger(x) \psi_b(0) \psi_a(0) \rangle$. In the topological phase we find that both decay *algebraically* and exhibit a revival at the edge, see Fig. 2 (c). This observation confirms the description of the topological phase via attributing a mass to the θ_- field. Finally, the symmetric sector can be described by a Luttinger liquid with a linear low-energy spectrum. This behavior is confirmed by the DMRG analysis: The finite size gap in a system of length L decays algebraically with $1/L$, see Fig. 2 (d). The variance of energy lies between $\frac{\Delta E}{|E|} = 3.7 \cdot 10^{-4}$ for the ground state calculations on short chains and $1.3 \cdot 10^{-3}$ for the excited state calculations on long chains. Note that ΔE is a measure of the maximal error of the gap. We can expect the results to be more accurate due to error cancellation as DMRG is variational. Therefore the errors in the ground state energy and the first excited state energies cancel to some extent when computing the gap. The same argument applies to Fig. 3 (c).

This is in contrast to the exactly solvable point at $u = g = w = 1$, where the low-energy spectrum is quadratic and the gap closes as $1/L^2$ [23]. This exactly solvable point is therefore a critical point and characterizes the phase transition from the topological phase towards phase separation, see below.

Decreasing the Luttinger parameter $K_- < 1$ eventually leads to a **gapless Luttinger liquid** (LL), where the operator (7) becomes irrelevant. This phase is characterized by an algebraic decay of all correlation functions and a unique ground state, see Fig. 1.

At half filling, two additional operators can become relevant and account for Umklapp processes. Both the inter- and intra-chain density-density interactions give

rise to these processes and two distinct and potentially relevant terms arise. The first one is the intra-chain Umklapp scattering

$$\left(\psi_{R\sigma}^\dagger \psi_{L\sigma}\right)^2 + \text{h.c.} \propto \cos\left(\sqrt{8\pi K_+} \phi_+ \pm \sqrt{8\pi K_-} \phi_-\right) \quad (8)$$

which becomes relevant for $(K_+ + K_-) < 1$ and where the plus/minus sign corresponds to $\sigma = a/b$. It leads to the formation of a **charge-density wave (CDW+SDW)** in both wires and provides a gap in the symmetric and antisymmetric sector, i.e., the whole theory is gapped. Indeed, the DMRG results show the appearance of this phase for strong intra-chain repulsion, see Fig. 1, as expected from bosonization. Furthermore, we find both pair correlations $h^-(x)$ and $h^+(x)$ decaying exponentially, indicating that both ϕ_- and ϕ_+ are well described as massive fields. The charge-density wave can also be directly seen in the local fermion density $\langle n_i^\sigma \rangle$, see Fig. 3 (b).

The second Umklapp process arises due to inter-chain density-density interactions

$$\left(\psi_{La}^\dagger \psi_{Ra}\right)^2 \left(\psi_{Lb}^\dagger \psi_{Rb}\right)^2 + \text{h.c.} \propto \cos\left(\sqrt{32\pi K_+} \phi_+\right). \quad (9)$$

It becomes relevant for $K_+ < 1/4$ and leads to a second type of **charge density wave (CDW)**. Here, only the symmetric sector becomes gapped which manifests in only the correlation function $h^+(x)$ decaying exponentially whereas $h^-(x)$ shows algebraic behavior, see Fig. 3 (a). As expected, this phase appears for varying the strength of the inter-chain interactions g . The transition from the topological to the LL and CDW phases is described by a Kosterlitz-Thouless transition and hence of second order; this is confirmed by the DMRG results.

Note that bosonization in principle would allow for an additional phase characterized by a spin density wave and driven by the operator

$$\left(\psi_{La}^\dagger \psi_{Ra}\right)^2 \left(\psi_{Rb}^\dagger \psi_{Lb}\right)^2 + \text{h.c.} \propto \cos\left(\sqrt{32\pi K_-} \phi_-\right). \quad (10)$$

which originates from the inter-chain density-density repulsion $n_i^a n_i^b n_{i+1}^a n_{i+1}^b$ contained in B_i^2 . This operator is relevant for $K_- < \frac{1}{4}$. Recall that here the spin density wave is driven by a four-body interaction whereas a general two-body inter-chain density-density interaction would become relevant for $K_- < 1$. Within our DMRG analysis, we did not find such a spin density phase.

Finally, two types of **phase separation** are observed for strong attractive interactions: For strong intra-chain attraction ($u > 0$), the phase separation occurs *on* the chains (PS), such that the fermions cluster on each chain while the particle number on both chains remains the same. The critical point $u = g = w = 1$ is located on the phase boundary between the intra-chain phase separation and the topological phase. For a large, negative inter-chain density-density interaction g , on the other hand,

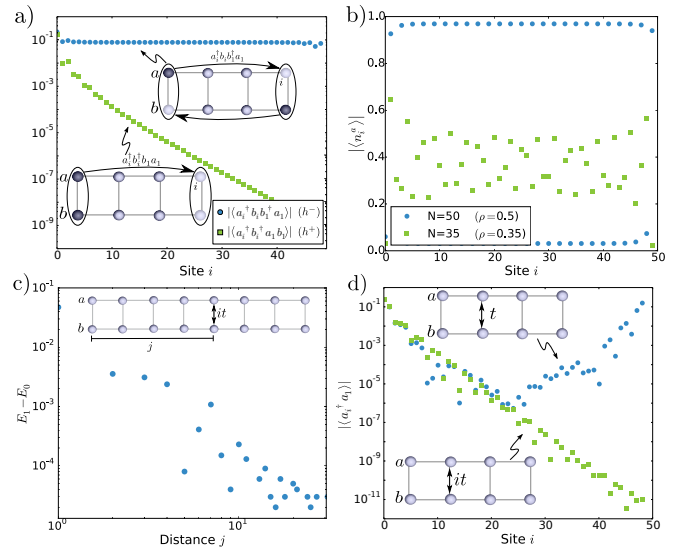


FIG. 3. (a) Inter-chain two-point functions h^\pm for a chain of length $L = 50$ with open boundaries for $u = -0.5$, $g = -1$ and $w = 1$ at half filling in the $\alpha = -1$ sector, indicating the existence of a gap only in the symmetric sector. The energy accuracy is $\frac{\Delta E}{|E|} = 2.3 \cdot 10^{-5}$. (b) Local density for a chain of length $L = 50$ with open boundaries for $u = g = -4$, $w = 1$ in the $\alpha = -1$ sector indicating the charge density wave. Accuracy of energy is $\frac{\Delta E}{|E|} = 6.8 \cdot 10^{-8}$ ($N = 50$) and $\frac{\Delta E}{|E|} = 2.2 \cdot 10^{-3}$ ($N = 35$). Note that the accuracy for $N = 50$ is much higher as the CDW+SDW state has an especially low entanglement entropy. (c) Dependence of the ground state energy splitting $E_1 - E_0$ in the presence of a local time-reversal breaking single-particle inter-chain hopping of strength $t = 0.05$ as a function of the distance j from the edge. Results are for an open chain of length $L = 61$ with $N = 43$ particles and $u = g = 0.9$, $w = 1$. Here, the energy error lies between $\frac{\Delta E}{|E|} = 9.6 \cdot 10^{-5}$ and $5.6 \cdot 10^{-4}$. (d) On-chain Green's function for an open chain of length $L = 50$ with $u = g = 0.9$, $w = 1$ at half filling in the presence of *global* single-particle hopping of strength $t = 0.05$ with (circles, $\frac{\Delta E}{|E|} = 4.4 \cdot 10^{-4}$) and without (squares, $\frac{\Delta E}{|E|} = 5.3 \cdot 10^{-5}$) time-reversal symmetry.

one finds an inter-chain phase separation (F), as the interaction now favors all fermions clustering on one chain while the other chain is empty, see Fig. 1. The transition from the topological phase to phase separation is of first order, as supported by the numerical analysis.

Symmetry breaking and disorder: Topological order manifests itself in a ground state degeneracy which is stable against disorder and symmetry-conserving perturbations. Using DMRG, we find that the ground state degeneracy and the degeneracy of the entanglement spectrum indeed are unaffected by disorder. Here, we implement disorder on the parameters u, g and w by making them site-dependent as $u_i = p_i u$ where $p_i \in [1 - \delta, 1 + \delta]$ are uniformly distributed random numbers and δ is the disorder strength. The parameters w and g are treated analogously. For a moderate disorder of $\delta = 0.15$, the

degeneracy of the entanglement spectrum remains unaffected in the topological phase, indicating its stability. The corresponding DMRG results are given in the appendix.

On the other hand, a natural perturbation breaking the subchain parity symmetry is single particle inter-chain hopping $a_i^\dagger b_i + \text{h.c.}$. However, it was argued in Ref. [23] that a residual time-reversal symmetry is sufficient to protect the topological phase at the critical point $u = g = w = 1$. This behavior is confirmed within our bosonization approach: A generic, local single-particle hopping between the two chains takes the form

$$P_\gamma(x) = e^{i\gamma} \psi_a^\dagger(x) \psi_b(x) + e^{-i\gamma} \psi_b^\dagger(x) \psi_a(x) \quad (11)$$

with a phase factor $\gamma \in [0, 2\pi)$. In the topological phase, a time-reversal *symmetric* perturbation ($\gamma = 0$) leads to exponentially decaying correlations $\langle P_\gamma(x) P_\gamma(0) \rangle$, whereas a time-reversal symmetry *breaking* perturbation ($\gamma \neq 0$) leads to an algebraic decay. We can confirm this prediction within our DMRG analysis by studying the ground state properties under perturbations of the form (11). Breaking time-reversal symmetry induces a ground state splitting which decays with the distance of the perturbation from the edge, see Fig. 3 (c). In contrast, for time reversal symmetric hopping, even a homogenous perturbation leaves the topological phase intact, with ground state degeneracy and revival of the Green's function at the edge, see Fig. 3 (d). The numerical results for the topological phase impressively certify its stability against perturbations violating subchain-parity conservation, as expected from bosonization and predicted at the critical point [23]. Finally, we would like to point out that for negative coupling w the role of these perturbations is reversed. This can be seen from the action of the gauge transformation on the time-reversal symmetry operator.

Conclusion: We investigated a model of interacting fermions in one dimension using bosonization and DMRG, explicitly demonstrating the stability of the topological properties of its exactly solvable, critical point against certain perturbations. We numerically computed the phase diagram of the model, featuring a variety of occurring phases that can be characterized by bosonization. The stability of the topological properties was demonstrated and we find them to be robust even in the presence of perturbations violating subchain-parity conservation. Nevertheless, we find that an additional symmetry (e.g., time-reversal) is required for an exponential splitting of the ground state degeneracy, while a generic setup with only particle number conservation shows an algebraic splitting.

We acknowledge support by the European Union under the ERC consolidator grant SIRPOL (grant N. 681208), and the Deutsche Forschungsgemeinschaft (DFG) within SFB/TRR 21. This research was supported in part by

the National Science Foundation under Grant No. NSF PHY-1125915.

APPENDIX

Bosonized Hamiltonian: To analyze the Hamiltonian qualitatively using bosonization, we separate the original Hamiltonian (1) into

$$H = H_0 + H_1 + H_2 + H_3, \quad (12)$$

and treat the continuum limit of the lattice model to allow for the field-theoretical description. Here, H_0 is the kinetic part, describing free fermions with the well known bosonized form [32]

$$H_0 = \frac{1}{2} \sum_{\eta=+,-} \int dx (\partial_x \theta_\eta)^2 + (\partial_x \phi_\eta)^2, \quad (13)$$

and H_1 , H_2 and H_3 are the intra-chain density-density interaction, the pair-hopping interaction and the inter-chain density-density interaction, respectively. These interactions are now treated perturbatively using bosonization and renormalization group arguments. The Fermi velocity is set to 1.

The bosonized form of the intra-chain density-density interaction is equally well studied [26, 27] and has the bosonized form

$$H_1 = \frac{u}{4\pi} \sum_{\sigma} \int dx \left(\frac{1}{2} + \sin^2(k_F a) \right) (\partial_x \phi_{\sigma})^2 + \left(\frac{1}{2} - \sin^2(k_F a) \right) (\partial_x \theta_{\sigma})^2, \quad (14)$$

away from half filling. Here k_F is the Fermi wavenumber encoding the filling of the system. By rescaling of the fields, H_1 can be absorbed into H_0 [27] leading to

$$\mathcal{H}_{0+1,c} = \sum_{\eta=\pm} \frac{\nu}{2} \left[K_{\eta} (\partial_x \theta_{\eta})^2 + \frac{1}{K_{\eta}} (\partial_x \phi_{\eta})^2 \right], \quad (15)$$

with the new parameters

$$K_{\eta} = \sqrt{\frac{1 + \frac{u}{4\pi} (1 + 2 \sin^2(k_F a))}{1 + \frac{u}{4\pi} (1 - 2 \sin^2(k_F a))}} \quad (16a)$$

$$\nu = 2 \sqrt{1 + \frac{2u}{4\pi} + \frac{u^2}{16\pi^2} (1 - 4 \sin^4(k_F a))}. \quad (16b)$$

The parameters K_{\pm} are effectively treated by a rescaling of the fields such that $H_0 + H_1$ regains the form of H_0 . That is,

$$\phi_{\pm} \mapsto \frac{1}{\sqrt{K_{\pm}}} \phi_{\pm} \quad (17a)$$

$$\theta_{\pm} \mapsto \sqrt{K_{\pm}} \theta_{\pm}. \quad (17b)$$

Note that although $K_+ = K_-$ while treating all interactions perturbatively in lowest order, this is not strictly fulfilled; especially not when going towards strong interactions, as can be seen from the DMRG results.

The pair hopping interaction term is known from studies of microscopic models of topologically ordered systems [16, 22] and has (away from half filling) the bosonized form

$$\begin{aligned} \mathcal{H}_2 = & q_1 \cos \left(\sqrt{8\pi/K_-} \theta_- \right) \\ & + q_2 \cos \left(\sqrt{8\pi} \left(\sqrt{1/K_-} \theta_- + \sqrt{K_-} \phi_- \right) \right) \\ & + q_3 \cos \left(\sqrt{8\pi} \left(\sqrt{1/K_-} \theta_- - \sqrt{K_-} \phi_- \right) \right), \end{aligned} \quad (18)$$

with $q_i \sim w$. When treating the interaction perturbatively and considering the behaviour of the couplings q_i under renormalization group, it turns out that the second and third terms have scaling dimension $\Delta = 2 \left(K_- + \frac{1}{K_-} \right)$ and are therefore never relevant, whereas the first term has scaling dimension $\Delta = \frac{2}{K_-}$ and becomes relevant for $K_- > 1$. What remains is the famous sine-Gordon model [33] which has been shown to refermionize to a system exhibiting topological order, with the continuum version of the Kitaev chain being a special case at $K_- = 2$ [16].

The inter-chain density-density interaction decomposes into intra-chain two-body interactions which are of the same form as H_1 and can hence be absorbed into H_0 by rescaling the fields, plus the three- and four-body inter-chain interactions.

We start from the bosonization of the full lowest order continuum limit of the pair interaction $n_i^{\sigma} n_{i+1}^{\sigma}$ which is

$$U_{\sigma} = V_{\sigma} + M_{\sigma} + F_{\sigma}, \quad (19)$$

with the notation

$$V_{\sigma} = (\psi_{R\sigma}^{\dagger} \psi_{R\sigma})^2 + (\psi_{L\sigma}^{\dagger} \psi_{L\sigma})^2 + 4 \sin^2(k_F a) \psi_{R\sigma}^{\dagger} \psi_{R\sigma} \psi_{L\sigma}^{\dagger} \psi_{L\sigma} \quad (20a)$$

$$M_{\sigma} = e^{2ik_F x} \psi_{L\sigma}^{\dagger} \psi_{R\sigma} (1 + e^{2ik_F a}) + \text{h.c.} \quad (20b)$$

$$F_{\sigma} = e^{4ik_F x + 2ik_F a} \left(\psi_{L\sigma}^{\dagger} \psi_{R\sigma} \right)^2 + \text{h.c.} \quad (20c)$$

Away from half filling, the four-body interaction then reads in its bosonized form

$$\begin{aligned} H_3^{4\text{-body}} = & g \int dx U_a(x) U_b(x) \\ = & \int dx V_a V_b + M_a M_b + F_a F_b. \end{aligned} \quad (21)$$

From equation (20a) follows that $V_a V_b$ has scaling dimension $\Delta = 4$ and is hence always irrelevant. When considering the three-body term, we find that the relevant part is

$$H_3^{3\text{-body}} = -g \int dx M_a M_b. \quad (22)$$

Thus, the contribution $M_a M_b$ precisely cancels and the inter-chain density-density interaction reduces to the potentially relevant term

$$F_a F_b = \left(\psi_{La}^\dagger \psi_{Ra} \right)^2 \left(\psi_{Rb}^\dagger \psi_{Lb} \right)^2 + \text{h.c.} \\ \propto \cos \left(\sqrt{32\pi K_-} \phi_- \right). \quad (23)$$

In the special case of half filling, two additional relevant terms appear, as certain oscillating terms do not average out anymore.

These are the on-chain umklapp scattering

$$\left(\psi_{Ra/b}^\dagger \psi_{La/b} \right)^2 + \text{h.c.} \\ \propto \cos \left[\sqrt{8\pi} \left(\sqrt{K_+} \phi_+ \pm \sqrt{K_-} \phi_- \right) \right], \quad (24)$$

which comes from the intra-chain density-density interaction terms and has scaling dimension $\Delta = 2(K_+ + K_-)$. In the domain of relevance, it is driving the system towards charge-density wave order on both chains simultaneously.

The second term is the inter-chain umklapp scattering arising from the four-body interaction which reads

$$\left(\psi_{La}^\dagger \psi_{Ra} \right)^2 \left(\psi_{Lb}^\dagger \psi_{Rb} \right)^2 + \text{h.c.} \\ \propto \cos \left(\sqrt{32\pi K_+} \phi_+ \right). \quad (25)$$

It has scaling dimension $\Delta = 8K_+$ and can open a gap exclusively in the symmetric sector.

Evaluation of the phase diagram: The color code of Fig. 1 in the main text is constructed from the DMRG ground state calculations in both subchain parity sectors using the gap between the sectors, $|E_0^{\alpha=1} - E_0^{\alpha=-1}|$, the ratio of minimum to maximum on-chain density $\langle n_i^a \rangle$

$$\Delta n = \frac{\min \{ \langle n_i^a \rangle \}}{\max \{ \langle n_i^a \rangle \}}, \quad (26)$$

the revival of the Green's function

$$v = \frac{\langle c_L^\dagger c_1 \rangle}{\langle c_1^\dagger c_1 \rangle}, \quad (27)$$

the minimum of that correlation function's envelope m , the mean fluctuation of $\langle n_i^a \rangle$,

$$f = \langle | \langle n_i^a \rangle - \langle \langle n_i^a \rangle \rangle_i | \rangle_i, \quad (28)$$

where $\langle \rangle_i$ denotes the spatial average, the mean minimal density

$$a = \langle \min \{ n_i^a, n_i^b \} \rangle_i, \quad (29)$$

and the standard deviation of energy $\Delta E = \sqrt{\langle H^2 \rangle - \langle H \rangle^2}$. The two-point correlation functions h^\pm are not directly employed, but checked explicitly at exemplary points within the phases. The color (r, g, b) in RGB code is now attributed as follows:

1. If $f > \frac{1}{4}$ and $\Delta n < \frac{1}{50}$, we face a large variance in density that extends over the entire system. As all observed cases of charge-density waves have significantly larger Δn , we can safely attribute on-chain phase separation and set $(r, g, b) = (0, 1, 0)$.
2. If $f < \frac{3}{10}$ and $a < \frac{1}{5}$, there is little density fluctuation on the chains but a large difference between them, which qualifies for inter-chain phase separation and we set $(r, g, b) = (1, 0, 1)$.
3. If neither on- nor inter-chain phase separation are found, we set the color as follows:

$$r = e^{-|E_0^{\alpha=1} - E_0^{\alpha=-1}|} \\ g = \begin{cases} 0 & \text{if } m > \frac{1}{4} \\ 7v & \text{if } m < \frac{1}{4}, v < \frac{1}{10} \\ \frac{7}{10} + \frac{3}{10} \sin \left(\frac{\pi(v - \frac{1}{10})}{\frac{1}{10}} \right) & \text{else} \end{cases} \\ b = \begin{cases} 1 & \text{if } f > \frac{3}{5} \\ \frac{5}{3}f & \text{else} \end{cases} \quad (30)$$

The threshold values are empirically determined by explicitly considering the decisive correlations and densities in the respective domains in parameter space.

The saturation is then used to represent the accuracy in form of the standard deviation of energy ΔE : It is set to $e^{-30\Delta E}$, that is, if the result is an exact eigenstate, it is $\Delta E = 0$ and therefore the saturation is 1, else it decays exponentially with the standard deviation.

Using this coloring scheme, we can visualize the different phases, as the phase separation is identified directly, the CDW+SDW phase features large on-chain density fluctuations but neither revival nor a degeneracy with respect to α and thus appears blue, the CDW phase does have a homogeneous density and no revival, but the groundstate is degenerate with respect to α , it hence appears red. The topological phase also has a homogeneous density, but features revival and ground state degeneracy and therefore is colored yellow. The LL phase does not have any of the probed characteristics and hence appears grey.

Additional DMRG results: The data presented here illustrates some of the properties and characteristics of the phases. The phase separation (both on the chains and between the chains) can directly be seen from the local fermion density $\langle n_i^{a/b} \rangle$, as shown in Fig. 4 (a) and (b). The entanglement entropy in these states is extremely low, as shown in Fig. 4 (c), such that they can be pictured as being close to product states and hence eigenstates of the local particle number operators. Note that such product states cannot be eigenstates of the model Hamiltonian due to the kinetic term, but the energy variance is sufficiently low here [with $(\Delta E)^2 = 6.28 \cdot 10^{-9}$ for the on-chain phase separation and $(\Delta E)^2 = 7.13 \cdot 10^{-10}$

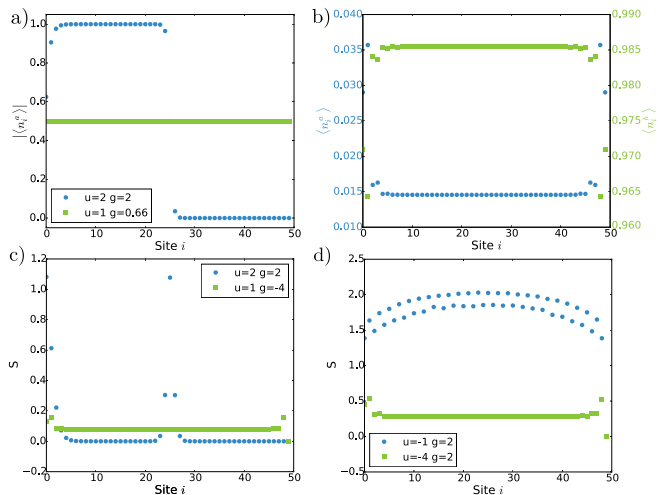


FIG. 4. (a) Local fermion density on one chain for the topological phase at $w = 1$, $u = 1$, $g = 0.66$ ($\frac{\Delta E}{|E|} = 0.0124$) and the phase separation at $w = 1$, $u = g = 2$ ($\frac{\Delta E}{|E|} = 2.676 \cdot 10^{-8}$) at half filling for two chains of length 50. With the fermion numbers being close to 1 and 0 in the phase separation, these values can be interpreted as eigenvalues. (b) Local fermion densities on both chain a (blue) and b (green) in the inter-chain phase separation at $w = 1$, $u = 1$, $g = -4$ at half filling for two chains of length 50 ($\frac{\Delta E}{|E|} = 1.375 \cdot 10^{-5}$). Again, the fermion numbers being close to 1 and 0 gives a low entanglement phase. (c) Entanglement entropy in the phase separation for on-chain (blue) and inter-chain (green) phase separation as a function of the bipartition site. The peaks in the entanglement entropy of the on-chain phase separated state stem from the transition between the entirely filled to the empty region. (d) Entanglement entropy in the full charge-density wave (green) ($\frac{\Delta E}{|E|} = 4.625 \cdot 10^{-8}$) and in the Luttinger liquid (blue) ($\frac{\Delta E}{|E|} = 4.969 \cdot 10^{-4}$) as a function of the bipartition site.

for the inter-chain phase separation] so that these states are close to the true groundstate.

The area law for entanglement entropy [34] in one-dimensional systems demands a constant entanglement entropy for gapped, one-dimensional Hamiltonians. As the bosonization predicts a full gap in the CDW+SDW phase, we therefore expect a constant entanglement entropy in this case, which is found in DMRG calculations as depicted in Fig. 4 (d). For comparison, we also show the entanglement entropy of the gapless Luttinger liquid phase that clearly varies with the subsystem size.

Also, the Luttinger liquid phase is characterized by a non-degenerate groundstate, as shown in the phase diagram in Fig. 1 of the main text, and algebraically decaying correlations as shown in Fig. 5 (a) — which corresponds to the system being gapless in both sectors.

Adding a weak local single-particle inter-chain hopping does not break the topologically ordered phase. This is not limited to the perturbation being local: A global single-particle hopping has the same effect, as shown in

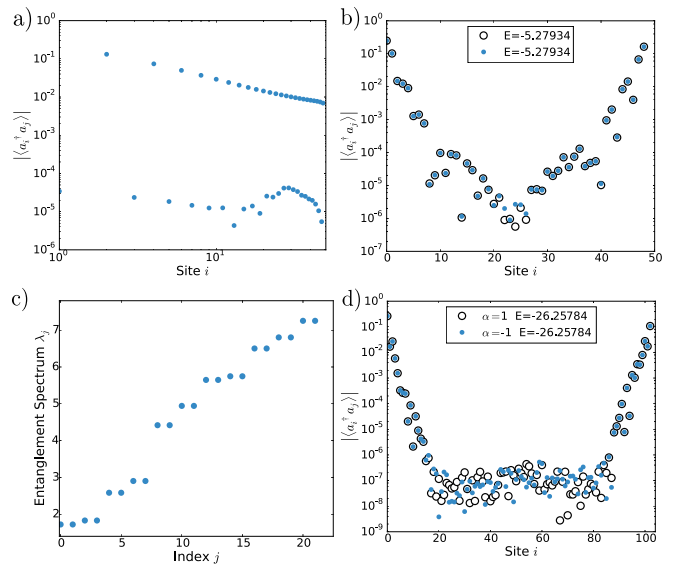


FIG. 5. (a) On-chain Green's function in the Luttinger liquid phase at $w = 1$, $u = -1$, $g = 2$ at half filling for two chains of length 50 ($\frac{\Delta E}{|E|} = 4.969 \cdot 10^{-4}$). The oscillatory behaviour of the correlation function leads to half of the datapoints being located at low values, but the algebraic decay of the envelope is clearly visible which connects to the phase being gapless in both sectors. (b) On-chain Green's function in the topological phase at $w = 1$, $u = g = 0.9$ for two chains of length 50 with a fermion number of 35 in the presence of a global single-particle hopping of strength $t = 0.05$ ($\frac{\Delta E}{|E|} = 4.43 \cdot 10^{-4}$). (c) Entanglement spectrum for the topological phase at $w = 1.1$, $u = g = 0.8$ ($\frac{\Delta E}{|E|} = 3.32 \cdot 10^{-4}$) for a bipartition at site $i = 64$ with the total chain length 104 and the particle number 93. Here, a disorder of $\delta = 15\%$ in all parameters is applied. The double degeneracy is clearly visible, indicating stability against spatial disorder. (d) Green's function and ground state degeneracy for the same system, showing the robustness of the edge state against disorder.

Fig. 5 (b), i.e., both the ground state degeneracy and the exponentially localized edge states remain stable in the presence of global weak single-particle inter-chain hopping. This is not the case if the single-particle hopping breaks time-reversal symmetry; then even a local perturbation can destroy the edge states.

The stability of the topological phase against disorder manifests directly in the stability of the degeneracy of the ground states and the entanglement spectrum as well as the exponential decay of the Green's function with a revival at the other end of the chain. This can be seen exemplarily in Fig. 5 (c) and (d), showing the entanglement spectrum and the Green's function which features the characteristic revival even in the presence of disorder.

DMRG Implementation: We implemented the DMRG algorithm using C++11 and utilizing the BLAS [35], LAPACK [36] and Arpack [37] libraries. We therefore make use of the BLAS and LAPACK routines and their respective C interface from Intel[®] MKL and

the Arpack++ C++ wrapper for Arpack [38]. The code is parallelized for shared memory architectures using openMP.

-
- * guther@itp3.uni-stuttgart.de; Current address: Max-Planck-Institute for Solid State Research, Heisenbergstraße 1, 70569 Stuttgart, Germany
- [1] D. J. Thouless, M. Kohmoto, M. P. Nightingale, and M. den Nijs, “Quantized hall conductance in a two-dimensional periodic potential,” *Phys. Rev. Lett.*, vol. 49, pp. 405–408, Aug 1982.
 - [2] X. Wen, “Topological orders and edge excitations in fractional quantum hall states,” *Advances in Physics*, vol. 44, no. 5, pp. 405–473, 1995.
 - [3] A. Kitaev, “Fault-tolerant quantum computation by anyons,” *Annals of Physics*, vol. 303, no. 1, pp. 2 – 30, 2003.
 - [4] C. Nayak, S. H. Simon, A. Stern, M. Freedman, and S. Das Sarma, “Non-abelian anyons and topological quantum computation,” *Rev. Mod. Phys.*, vol. 80, pp. 1083–1159, Sep 2008.
 - [5] D. A. Ivanov, “Non-abelian statistics of half-quantum vortices in p -wave superconductors,” *Phys. Rev. Lett.*, vol. 86, pp. 268–271, Jan 2001.
 - [6] A. Y. Kitaev, “Unpaired majorana fermions in quantum wires,” *Physics-Uspekhi*, vol. 44, no. 10S, p. 131, 2001.
 - [7] D. Asahi and N. Nagaosa, “Topological indices, defects, and majorana fermions in chiral superconductors,” *Phys. Rev. B*, vol. 86, p. 100504, Sep 2012.
 - [8] N. Read and D. Green, “Paired states of fermions in two dimensions with breaking of parity and time-reversal symmetries and the fractional quantum hall effect,” *Phys. Rev. B*, vol. 61, pp. 10267–10297, Apr 2000.
 - [9] Y. Ran, Z. Yi, and A. Vishwanath, “One-dimensional topologically protected modes in topological insulators with lattice dislocations,” *Nature Physics*, vol. 5, pp. 298–303, 2009.
 - [10] L. Rokhinson, X. Liu, and J. Furdyna, “The fractional a.c. josephson effect in a semiconductor-superconductor nanowire as a signature of majorana particles,” *Nature Physics*, vol. 8, no. 11, pp. 795–799, 2012.
 - [11] A. Das, Y. Ronen, Y. Most, Y. Oreg, M. Heiblum, and H. Shtrikman, “Zero-bias peaks and splitting in an al–inas nanowire topological superconductor as a signature of majorana fermions,” *Nature Physics*, vol. 8, no. 12, pp. 887–895, 2012.
 - [12] M. T. Deng, C. L. Yu, G. Y. Huang, M. Larsson, P. Caroff, and H. Q. Xu, “Anomalous zero-bias conductance peak in a nb–insb nanowire–nb hybrid device,” *Nano Letters*, vol. 12, no. 12, pp. 6414–6419, 2012. PMID: 23181691.
 - [13] S. Albrecht, A. Higginbotham, M. Madsen, F. Kuemmeth, T. Jespersen, J. Nygård, P. Krogstrup, and C. Marcus, “Exponential protection of zero modes in majorana islands,” *Nature Physics*, vol. 531, no. 7593, pp. 206–209, 2016.
 - [14] V. Mourik, K. Zuo, S. M. Frolov, S. R. Plissard, E. P. A. M. Bakkers, and L. P. Kouwenhoven, “Signatures of majorana fermions in hybrid superconductor-semiconductor nanowire devices,” *Science*, vol. 336, no. 6084, pp. 1003–1007, 2012.
 - [15] S. Nadj-Perge, I. K. Drozdov, J. Li, H. Chen, S. Jeon, J. Seo, A. H. MacDonald, B. A. Bernevig, and A. Yazdani, “Observation of majorana fermions in ferromagnetic atomic chains on a superconductor,” *Science*, vol. 346, no. 6209, pp. 602–607, 2014.
 - [16] M. Cheng and H.-H. Tu, “Majorana edge states in interacting two-chain ladders of fermions,” *Phys. Rev. B*, vol. 84, p. 094503, 2011.
 - [17] L. Fidkowski, R. M. Lutchyn, C. Nayak, and M. P. A. Fisher, “Majorana zero modes in one-dimensional quantum wires without long-ranged superconducting order,” *Phys. Rev. B*, vol. 84, p. 195436, Nov 2011.
 - [18] J. D. Sau, B. I. Halperin, K. Flensberg, and S. Das Sarma, “Number conserving theory for topologically protected degeneracy in one-dimensional fermions,” *Phys. Rev. B*, vol. 84, p. 144509, Oct 2011.
 - [19] J. Ruhman, E. Berg, and E. Altman, “Topological states in a one-dimensional fermi gas with attractive interaction,” *Phys. Rev. Lett.*, vol. 114, p. 100401, Mar 2015.
 - [20] A. Keselman and E. Berg, “Gapless symmetry-protected topological phase of fermions in one dimension,” *Phys. Rev. B*, vol. 91, p. 235309, Jun 2015.
 - [21] G. Ortiz, J. Dukelsky, E. Cobanera, C. Esebbag, and C. Beenakker, “Many-body characterization of particle-conserving topological superfluids,” *Phys. Rev. Lett.*, vol. 113, p. 267002, Dec 2014.
 - [22] C. V. Kraus, M. Dalmonte, M. A. Baranov, A. M. Läuchli, and P. Zoller, “Majorana edge states in atomic wires coupled by pair hopping,” *Phys. Rev. Lett.*, vol. 111, p. 173004, Oct 2013.
 - [23] N. Lang and H. Büchler, “Topological states in a microscopic model of interacting fermions,” *Phys. Rev. B*, vol. 92, p. 041118, Jul 2015.
 - [24] F. Iemini, L. Mazza, D. Rossini, R. Fazio, and S. Diehl, “Localized majorana-like modes in a number-conserving setting: An exactly solvable model,” *Phys. Rev. Lett.*, vol. 115, p. 156402, Oct 2015.
 - [25] D. Matthies and E. Lieb, “Exact solution of a many-fermion system and its associated boson field,” *Journal of Mathematical Physics*, vol. 6, 1965.
 - [26] J. von Delft and H. Schoeller, “Bosonization for beginners - refermionization for experts,” *Annalen der Physik*, vol. 7, no. 4, 1998.
 - [27] D. Sénéchal, “An introduction to bosonization,” *eprint arXiv:cond-mat/9908262*, Aug. 1999.
 - [28] S. R. White, “Density matrix formulation for quantum renormalization groups,” *Phys. Rev. Lett.*, vol. 69, pp. 2863–2866, Nov 1992.
 - [29] S. R. White and D. A. Huse, “Numerical renormalization-group study of low-lying eigenstates of the antiferromagnetic $S = 1$ heisenberg chain,” *Phys. Rev. B*, vol. 48, pp. 3844–3852, Aug 1993.
 - [30] U. Schollwöck, “The density-matrix renormalization group in the age of matrix product states,” *Annals of Physics*, vol. 326, 2011.
 - [31] C. Hubig, I. P. McCulloch, U. Schollwöck, and F. A. Wolf, “Strictly single-site dmrg algorithm with subspace expansion,” *Phys. Rev. B*, vol. 91, p. 155115, Apr 2015.
 - [32] A. O. Golovinskiy, A. A. Nersisyan, and A. M. Tsvelik, *Bosonization and strongly correlated systems*. Cambridge: Cambridge University Press, 1998.
 - [33] S. Coleman, “Quantum sine-gordon equation as the massive thirring model,” *Phys. Rev. D*, vol. 11, pp. 2088–

- 2097, Apr 1975.
- [34] J. Eisert, M. Cramer, and M. B. Plenio, “Colloquium : Area laws for entanglement entropy,” *Rev. Mod. Phys.*, vol. 82, pp. 277–306, Feb 2010.
- [35] C. L. Lawson, R. J. Hanson, D. R. Kincaid, and F. T. Krogh, “Basic linear algebra subprograms for fortran usage,” *ACM Trans. Math. Softw.*, vol. 5, no. 3, pp. 308–323, 1979.
- [36] E. Anderson, Z. Bai, C. Bischof, S. Blackford, J. Demmel, J. Dongarra, J. D. Cruz, A. Greenbaum, S. Hammarling, A. McKenney, and D. Sorensen, *LAPACK Users’ Guide*. Philadelphia, PA: Society for Industrial and Applied Mathematics, third ed., 1999.
- [37] R. Lehoucq, K. Maschhoff, D. Sorensen, and C. Yang, “Arpack,” 1997.
- [38] F. Gomes and D. Sorensen, “Arpack++,” 2000.